Articles

Contribution from the Ecole de Chimie, 34075 Montpellier Cedex, France, Institut de Physique Nucléaire (et IN2P3), Université de Lyon I, 68622 Villeurbanne Cedex, France, Department of Chemistry and the Saskatchewan Accelerator Laboratory, University of Saskatchewan, Saskatoon, Saskatchewan S7N 0W0, Canada, and Bereich Strahlenchemie, Hahn-Meitner-Institut, Postfach 39 01 28, D-1000 Berlin 39

Theoretical Study by the Xα Method of Platinum(III) Complex Ions Containing Aquo and Chloro Ligands

A. Goursot,[1a] H. Chermette,[1b] W. L. Waltz,*[,1c] and J. Lilie[1d]

Received July 22, 1988

The "quasi" relativistic version of the multiple-scattering Xα molecular orbital model has been used to investigate possible structures for monomeric platinum(III) complex ions that contain aquo and chloro ligands. These species arise as transitory products in the pulse radiolysis of aqueous solutions containing tetrachloroplatinum(II), $[PtCl_4]^{2-}$, or hexachloroplatinum(IV), $[PtCl_6]^{2-}$, and in the flash photolysis of the platinum(IV) complex. Calculations have been performed on the electronic structures for model complex ions possessing tetra-, and penta-, and hexacoordination. In earlier studies, a 10-electron oxygen atom had been employed as a model for a water or hydroxide ligand, and more detailed calculations reported herein support the validity of this approximation for the visible charge-transfer absorption band; however, to account for the UV CT band, it is necessary to incorporate specifically the presence of an OH group. The results have been used to calculate the peak positions for the intense charge-transfer transitions occurring in the near-UV–visible regions in order to compare them to the experimentally observed absorption spectra. The close agreement between the observed and predicted bands supports the proposal that shorter lived species are six-coordinated, distorted-octahedral types such as $[PtCl_4(OH)(H_2O)]^{2-}$. The comparisons for the longer lived intermediates, formed from the decay of the six-coordinate entities, lead to the viewpoint that these species are best described within the framework of limiting square-planar forms as exemplified by $[PtCl_2(OH)_2]^-$.

Introduction

Photochemical and radiolytic studies of the square-planar tetrachloroplatinum(II) ion, $[PtCl_4]^{2-}$, the octahedral hexachloroplatinum(IV) ion, $[PtCl_6]^{2-}$, and congeneric halogen systems have played a prominent role in the development of inorganic photochemistry and radiation chemistry in both modern-day and historical senses.[2,3] For example the photosensitivity of $[PtCl_6]^{2-}$ has been known for over 150 years; however, it is now well-recognized that this behavior involves different processes: photoredox, photoaquation, and photoligand exchange.[2,4-8] The last two phenomena exhibit quantum yields well in excess of 1, indicating chain mechanisms where the results generally point to the carriers being labile, transitory platinum(III) species. Interest in such species is no longer confined to these situations but now includes a growing list such as the synthesis of organoplatinum(II) and -(IV) compounds and the deposition of metallic platinum.[9-11]

The developments of the fast reaction techniques of pulse radiolysis and flash-laser photolysis have afforded the means to generate and characterize in a more direct fashion platinum(III) transients.[12-17] This has led to the recognition that different reaction modes can give rise to the same or similar intermediates in aqueous media; for instance, the reaction of the hydroxyl radical with $[PtCl_4]^{2-}$ yields on the microsecond time scale a transient with an absorption peak near 450 nm that subsequently decays to give a longer lived species with a maximum at about 410 nm. This species (or closely related ones) appears in the reaction of $[PtCl_6]^{2-}$ with the hydrated electron and has been observed on the millisecond scale in the conventional flash photolysis of this platinum(IV) complex ion.[12,14] While in these earlier studies no direct evidence for a precursor(s) was found, more recent results now show that the platinum(III) transient absorbing at 410 nm is not the nascent product.[17,18]

The optical bands associated with such species are relatively intense ($\epsilon > 2000\ M^{-1}\ cm^{-1}$) and thus indicative of charge-transfer transitions (CT); however, the bands are also broad (fwhm ca. 50–80 nm) and devoid of fine structure. This latter feature plus the occurrence of a number of intermediates has made it difficult to characterize the precise natures of the platinum(III) species. Accompanying this uncertainty have been different putative compositions and structures: $[PtCl_6]^{3-}$ (distorted octahedron), $[PtCl_5]^{2-}$ (square pyramid, trigonal bipyramid) and $[PtCl_4]^-$ (square plane).[12-16]

In an effort to expand the viewpoints about these and related species, we have applied the "quasi" relativistic version of the multiple-scattering Xα molecular orbital model to calculate the positions of allowed CT transitions for comparison to the experimentally determined maxima. This method has proven to be successful in providing good descriptions of ligand-to-metal charge-transfer (LMCT) and photoelectron spectra for stable

* To whom correspondence should be addressed.

(1) (a) Ecole de Chimie. (b) Université de Lyon. (c) University of Saskatchewan. (d) Hahn-Meitner-Institut.
(2) Balzani, V.; Carassiti, V. *Photochemistry of Coordination Compounds*; Academic: London, 1970; Chapter 12.
(3) Buxton, G. V.; Sellers, R. M. *Coord. Chem. Rev.* **1977**, *22*, 195–274.
(4) Rich, R. L.; Taube, H. *J. Am. Chem. Soc.* **1954**, *76*, 2608–2611.
(5) Dreyer, R.; König, K.; Schmidt, H. *Z. Phys. Chem. (Leipzig)* **1964**, *227*, 257–271.
(6) Dreyer, R.; König, K. *Z. Chem.* **1966**, *6*, 271.
(7) Cox, L. E.; Peters, D. G.; Wehry, E. L. *J. Inorg. Nucl. Chem.* **1972**, *34*, 297–305.
(8) Shagisultanova, G. A.; Orisheva, R. M.; Karaban, A. A.; Gorbunova, S. P. *Russ. J. Inorg. Chem. (Engl. Transl.)* **1972**, *17*, 1646–1647; *Zh. Neorg. Khim.* **1972**, *17*, 3129.
(9) Shul'pin, G. B.; Nizova, G. V.; Lederer, P. *J. Organomet. Chem.* **1984**, *275*, 283–294.
(10) Shul'pin, G. B.; Nizova, G. V.; Nikitaev, A. T. *J. Organomet. Chem.* **1984**, *276*, 115–153.
(11) Cameron, R. E.; Bocarsly, A. B. *Inorg. Chem.* **1986**, *25*, 2910–2913.
(12) Adams, G. B.; Broszkiewicz, R. B.; Michael, B. D. *J. Chem. Soc., Faraday Trans. 1* **1968**, *64*, 1256–1264.
(13) Ghosh-Mazumdar, A. S.; Hart, E. J. *Int. J. Radiat. Phys. Chem.* **1969**, *1*, 165–176.
(14) Wright, R. C.; Laurence, G. S. *J. Chem. Soc., Chem. Commun.* **1972**, 132–133.
(15) Storer, D. K.; Waltz, W. L.; Brodovitch, J. C.; Eager, R. L. *Int. J. Radiat. Phys. Chem.* **1975**, *7*, 693–704.
(16) Brozkiewicz, R. K.; Grodkowski, J. *Int. J. Radiat. Phys. Chem.* **1976**, *8*, 359–365.
(17) Goursot, A.; Kirk, A. D.; Waltz, W. L.; Porter, G. B.; Sharma, D. K. *Inorg. Chem.* **1987**, *26*, 14–18.
(18) Waltz, W. L.; Lilie, J.; Goursot, A.; Chermette, H. *Inorg. Chem.*, following paper in this issue.

0020-1669/89/1328-2241$01.50/0

chloro complex ions of platinum and iridium.[19-23] To the extent that a successful comparison can be made between calculated and experimentally observed peaks for transient species of interest here, this provides insight into the composition and structure of the entity being observed: at a minimum, this exercise serves to limit the possibilities that need to be considered. With use of a 10-electron oxygen model for a hydroxide or aquo ligand, earlier calculations have led to the suggestion that the 450-nm species could be a distorted-octahedral system of the type $[Pt^{III}Cl_4O_2]$ and that $[PtCl_6]^{3-}$ with moderate elongation of the Pt–Cl_{ax} bonds and square-planar $[PtCl_4]^-$ were viable possibilities for entities exhibiting peaks near 290 and 410 nm, respectively.[24,25] Similar calculations have aided in the identification of the nascent, short-lived product (τ = 210 ps) found in the pulsed-laser photolysis of $[PtCl_6]^{2-}$ as being square-pyramidal $[PtCl_5]^{2-}$.[17]

In this paper and the accompanying experimental one,[18] we have endeavored to use the synergistic interplay between experiment and theory to expand and clarify the understanding of the natures of the observed platinum(III) complex ions. In part, this has been motivated by the general objective of determining the limits to which the Xα method can serve as a tool for structure elucidation of short-lived metal complexes but also by the need to reexamine some of our earlier proposals in light of new experimental findings. Specifically we focus here on the extent to which a 10-electron oxygen atom is a valid model for OH^- and H_2O ligands through the detailed consideration of five- and six-coordinate cases such as $[PtCl_4(OH)]^{2-}$ (C_s symmetry), *cis*- and *trans*-$[PtCl_3(OH)_2]^{2-}$ (C_s, C_{2v}) and *trans*-$[PtCl_4(OH)H_2O]^{2-}$ (C_s). In a related context, further consideration is given to the nature of the 410-nm transient. Earlier calculated results for square-planar $[PtCl_4]^-$ indicated the presence of two CT transitions, one at 410 nm and the other at 620 nm; however, we have been unable to detect the latter band in the 500–700-nm region. This finding in concert with conductivity results has led us to consider tetracoordinated complexes incorporating hydroxide (or aquo) ligands as models for the longer lived, 410-nm transient.

In these investigations, we have also attempted to account for deviations from regular geometries. Spectroscopic studies indicate excited-state distortions for d^6 and d^8 complexes; for example, the photoactive $^3T_{1g}$ and $^1T_{1g}$ states of $[Co(NH_3)_6]^{3+}$ and the emitting ligand field state of $[PtCl_4]^{2-}$.[26,27] In both instances, the Jahn–Teller excited states have one electron in an antibonding d_σ MO and are found to exhibit substantially increased bond lengths. Similarly, d^7 penta- and hexacoordinated Pt(III) models also have one electron in an antibonding d_σ orbital; thus, they are expected to have expanded bond lengths with respect to their d^6 counterparts. In contrast, the d^7 planar Pt(III) species have one less electron, in an antibonding d_π MO, compared to square-planar d^8 systems. Here some bond contraction relative to the length in d^8 Pt(II) complexes seems more probable. Our principal aim in considering deviations from regular geometries has not been to determine precise geometrical features but rather to use symmetry considerations and analysis of the effects of geometrical changes on the calculated CT transitions (essentially the energy shift of the σ antibonding HOMO) in order to select plausible structures for the transients. While these theoretical calculations do not take into account effects such as interactions of the complex ions with the surrounding solvent, they can nevertheless be very useful to the extent that the conclusions drawn from the CT calculations do support the experimental arguments. In this regard, the results derived here from theory and those obtained from experiment do yield a consistent picture as to the natures of the short- and long-lived platinum(III) intermediates.[18]

Computational Method

The "quasi" relativistic MS–Xα method has been employed.[28,29] The effects of the mass-velocity and Darwin corrections are included self-consistently, and those of the spin–orbit operator are neglected. The standard Pt–O and Pt–Cl bond lengths, determined experimentally for Pt(IV) complexes as 2.04 and 2.32 Å, respectively, are the same as those used previously.[24,25] Regular deviations from these values have been also included: 0.10, 0.15, 0.20, and 0.25 Å. Calculations with bond angle distortions of up to 10° (from 90 or 120°) have been performed. A possible deviation from planarity for the tetracoordinated $[PtCl_2(OH)_2]^-$ has been investigated. The penta- and hexacoordinated structures have been studied in C_{4v} symmetry where the C_4 axis is collinear with the z axis, and the $z0x$ and $z0y$ planes are σ mirror planes. The radii of the Pt, Cl, and O spheres are those used in our earlier work.[24,25] The values of the exchange parameters (α_{Pt} = 0.693 06, α_{Cl} = 0.723 25, α_O = 0.744 47) are those optimized by Schwarz,[30] and the exchange parameter for H (α_H = 0.777 25) is that proposed by Slater.[31] A weighted average of these atomic values has been chosen for the interatomic and extranuclear regions, and partial waves up to l = 4 are included in the MS expansion in the metal sphere, up to l = 1 in the Cl and O spheres, and up to l = 0 for the H sphere. The transition-state procedure has been employed in the evaluation of the excitation energies without the inclusion of spin polarization.[32] Spin–orbit coupling effects have been neglected because they vanish to first order for the ground state (GS) and CT states of the d^7 complexes of interest here. For these d^7 complexes that likely have doublet ground states, the observed CT bands exhibiting considerable intensities have been taken to be associated with spin-allowed transitions populating doublet CT excited states. In this context, only transitions from ligand MOs to the singly occupied HOMOs have been considered. A version of the extended Hückel (EH) method has also been used that includes two-body repulsion corrections,[33] and the valence-orbital ionization potentials employed are those given by Pensak and McKinney.[34]

Results and Discussion

I. General Remarks about the CT Transitions for Nonplanar Pt(III) Models (2–6). In octahedral d^6 complex ions, such as $[PtCl_6]^{2-}$, the allowed CT transitions are t_{1u}, $t_{2u} \rightarrow e_g$. As proposed by Jørgensen,[35,36] the very high intensity transitions are the $t_{1u} \rightarrow e_g$ ones. This arises in part because the symmetry orbital ($t_{1u}(\sigma)$) that is comprised of p_z orbitals from the axial ligands mixes with the symmetry orbital ($t_{1u}(\pi)$) that is based upon the p_z orbitals of the equatorial ligands, the latter being p_π orbitals whereas the axial ones are p_σ orbitals with the 0z axis being collinear with the C_4 axis. Maximum overlap occurs between the Pt d_{z^2} orbital (one component of the e_g MO) and the p_z orbitals of the axial ligands ($p_\sigma \rightarrow d_\sigma$, CT) whereas such overlap is negligible with the equatorial ligand p_z orbitals ($p_\pi \rightarrow d_\sigma$, CT). This proposal is in complete agreement with the results obtained from MS–Xα calculations for $[PtCl_6]^{2-}$.[20] Here the observed CT bands at 38 200 cm^{-1} (ϵ = 24 500 M^{-1} cm^{-1}) and 49 500 cm^{-1} (ϵ > 30 000 M^{-1} cm^{-1}) have been assigned to $3t_{1u} \rightarrow 3e_g$ (calculated at 37 900 cm^{-1}) and to $2t_{1u} \rightarrow e_g$ (calculated at 48 500 cm^{-1}), respectively. The analysis of the $3t_{1u}$ and $2t_{1u}$ MOs shows that $3t_{1u}$ results from a mixing of 40% $t_{1u}(\sigma)$ and 60% $t_{1u}(\pi)$ while $2t_{1u}$, which is related to the more intense band, is comprised of 62% $t_{1u}(\sigma)$ and 38% $t_{1u}(\pi)$. When the axial and equatorial ligands are different, as is the case in the present study, then t_{1u} is split under the low symmetry with the axial and equatorial ligand orbitals being separated into different MOs. In this situation, it seems reasonable to assume in view of the above that the CT transitions from the axial p_z orbitals to that of Pt d_{z^2} will be intense; by contrast, the ones

(19) Goursot, A.; Chermette, H. *Chem. Phys.* **1982**, *69*, 329–337.
(20) Goursot, A.; Penigault, E.; Chermette, H. *Chem. Phys. Lett.* **1983**, *97*, 215–220.
(21) Goursot, A.; Chermette, H.; Daul, C. *Inorg. Chem.* **1984**, *23*, 305–314.
(22) Goursot, A.; Chermette, H. *Can. J. Chem.* **1985**, *63*, 1407–1411.
(23) Ginsberg, A. P.; Osborne, J. H.; Sprinkle, C. R. *Inorg. Chem.* **1983**, *22*, 254–266.
(24) Goursot, A.; Chermette, H.; Penigault, E.; Chanon, M.; Waltz, W. L. *Inorg. Chem.* **1984**, *23*, 3618–3625.
(25) Goursot, A.; Chermette, H.; Chanon, M.; Waltz, W. L. *Inorg. Chem.* **1985**, *24*, 1042–1047.
(26) Wilson, R. B.; Solomon, E. I. *J. Am. Chem. Soc.* **1980**, *102*, 4085–4095.
(27) Viaene, L.; Ceulemans, A.; Vanquickenborne, L. G. *Inorg. Chem.* **1985**, *24*, 1713–1716.
(28) Johnson, K. H. *Adv. Quantum Chem.* **1973**, *7*, 143–185.
(29) Boring, M.; Wood, J. H. *J. Chem. Phys.* **1979**, *71*, 392–399.
(30) Schwarz, K. *Phys. Rev. B; Solid State* **1972**, *5*, 2466–2468.
(31) Slater, J. C. *Int. J. Quantum Chem.* **1973**, *S7*, 533.
(32) Slater, J. C. *Adv. Quantum Chem.* **1972**, *6*, 1–92.
(33) Anderson, A. B. *J. Chem. Phys.* **1975**, *62*, 1187–1188.
(34) Pensak, D. A.; McKinney, R. J. *Inorg. Chem.* **1979**, *18*, 3407–3413.
(35) Jørgensen, C. K. *Acta Chem. Scand.* **1956**, *10*, 518–534.
(36) Jørgensen, C. K. *Mol. Phys.* **1959**, *2*, 309–332.

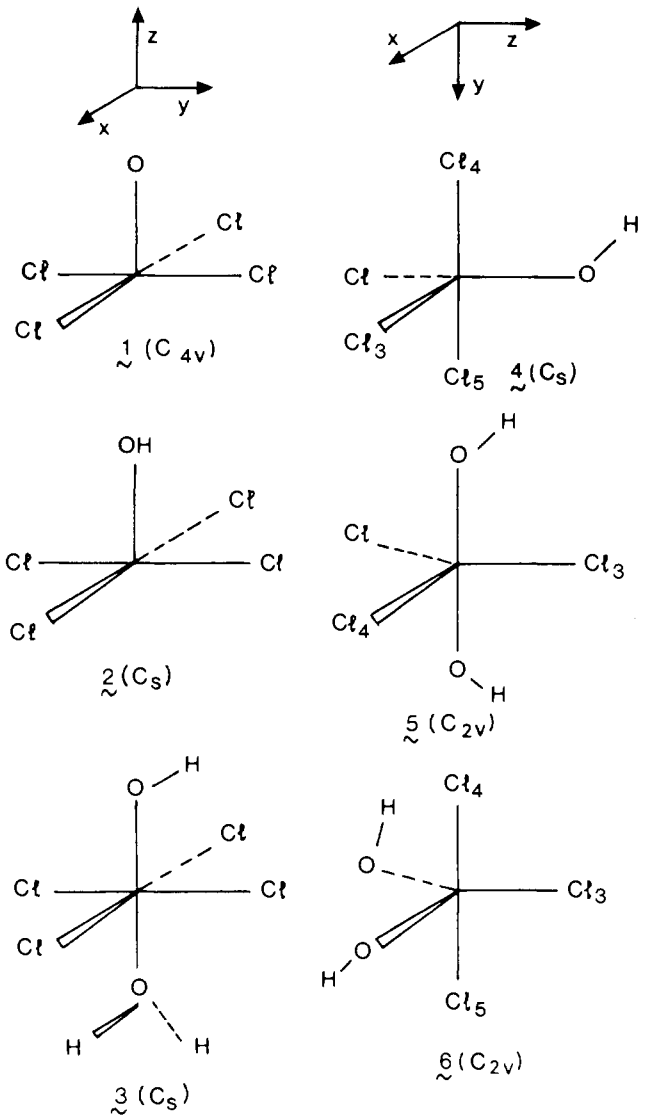

Figure 1. Hexa- and pentacoordinated structures.

involving the equatorial p_z orbitals should be weak.

In order to obtain more precise insight into these overlap arguments, the overlap integrals between the various ligand orbitals and those on the metal center that contribute to the HOMOs have been calculated by the EH method for the models **2**–**6** of Figure 1. All the nonzero values have been considered in the discussion below, and only *zero* overlap integrals as implied by symmetry or angular criteria have been used to eliminate a transition from further consideration. The conclusions drawn from the analysis of the EH overlap matrix elements for forms **2**–**6** indicate first of all that these models fall into two groups: the first is comprised of compounds **2** and **3** derived from C_{4v} symmetry with four chlorines in the $x0y$ plane, and the second group includes models **4**–**6**, where the ligands lie in a plane ($x0z$) and the two others reside on the y axis. For forms **2** and **3**, only Cl p_x, p_y and O p_z orbitals have a nonvanishing overlap with Pt $5d_{z^2}$ (HOMO).[37]

In the second group, the HOMOs for compounds **4a** (see below) and **6** have mixed Pt $5d_{z^2}$, $5d_{x^2-y^2}$ character; the HOMO of **4b** (see below) is Pt $5d_{xz}$, and that for **5** has degenerate Pt $5d_{z^2}$ and $5d_{xz}$ MOs. For these forms, the bond angles for HO–Pt–Cl and Cl–Pt–Cl are 120°, and one needs to take into account the overlaps of the Pt $5d_{z^2}$ or $5d_{z^2}$, $5d_{x^2-y^2}$ HOMO with the following ligand orbitals (see Figure 1): both p_x and p_z for the equatorial ligands that are not located on the 0z axis (**4a**, Cl_3; **5**, Cl_4; **6**, O); the p_z orbital of the ligand on the z axis (**4a**, O; **5** and **6**, Cl_3); the p_y orbitals of the ligands on the y axis (**4a** and **6**, Cl_4, Cl_5; **5**, O). For Pt $5d_{xz}$, overlap only occurs with orbitals involving the equatorial ligands: p_x of the ligand on the 0z axis (**4b**, O; **5** and **6**, Cl_3) and, for the other ligands, p_x and p_y (**4b**, Cl_3; **5**, Cl_4; **6**, O). Consideration of the foregoing features has assisted in the assignment of the CT transitions that are predicted to be intense, as discussed in the next section.

II. Models for Short-Lived Transient(s). New experimental results on the reaction of the hydroxyl radical and square-planar $[PtCl_4]^{2-}$ have now established several key facts.[18] The process involves OH addition, and the resulting platinum(III) intermediate exhibits two CT bands with peaks at 455 nm and near 260 nm: only the band at the longer wavelength had been identified in previous studies.[12,13] Furthermore, there are strong indications that the nascent product also has bound to it a water molecule. These features have oriented our study to the consideration of penta- and hexacoordinated structures $[PtCl_4O]^{3-}$, $[PtCl_4(OH)]^{2-}$, and $[PtCl_4(OH)(H_2O)]^{2-}$ and in so doing to reexamine an earlier use of a 10-electron oxygen atom as a model for a hydroxo or aquo ligand.[25]

To test this approximation, the electronic structure and CT spectrum of $[PtCl_4O]^{3-}$ (Figure 1, form **1**) have been compared to those of $[PtCl_4(OH)]^{2-}$, possessing a nonlinear Pt–O–H unit (**2** of Figure 1, C_s symmetry). Here the influence of the OH orientation with respect to the chlorines has been checked by performing two separate calculations for different hydrogen positions, either in a Cl,Pt,O plane or in the bisector plane of a Cl–Pt–Cl angle; however, the differences in the calculated CT transitions are negligible, as they amount to less than 800 cm^{-1}.

The upper valence MOs for $[PtCl_4O]^{3-}$ (C_{4v}) and for $[PtCl_4(OH)]^{2-}$ (C_s) are shown in Figure 2: these diagrams correspond to calculations performed with increased Pt–Cl and Pt–O bond lengths, 2.48 and 2.30 Å, respectively. The HOMOs for both structures involve strong antibonding interactions between Pt and O because both MOs have 50% character for Pt d_{z^2} and for O p_σ. In the C_s model, the antibonding d_π–O p_π MOs are stabilized with respect to the HOMO, but for both structures **1** and **2**, one finds a ligand MO localized on the O sphere that is located among the Cl p_π levels (Figure 2).

The presence of this MO is a critical feature in the calculated CT spectrum because, as shown by the EH findings, the only nonzero overlaps occur between the Pt $5d_{z^2}$ CT orbital and those of O p_z and Cl p_x, p_y. Moreover, the O $2p_z \rightarrow$ Pt $5d_{z^2}$ CT is certainly associated with an intense absorption band. According to the criteria proposed by Day and Sanders,[38] the intense CT transitions are those for which the electron movement and the electric dipole are parallel. This indicates that only the transitions leading to $^2A_1$ or $^2A'$ in C_{4v} or C_s symmetry, respectively, need to be considered: the electron flow during the CT transition is directed along the 0z axis. In C_s symmetry, combinations of Cl p_x orbitals are the sole bases for the a″ irreducible representation, and so only the O $2p_z \rightarrow$ Pt $5d_{z^2}$ transitions (a′ → a′ and $p_\sigma \rightarrow d_\sigma$ CT type) need be considered for cases **2** and **3**. The values calculated for these transitions are presented in Table I for $[PtCl_4O]^{3-}$ (**1**) and $[PtCl_4(OH)]^{2-}$ (**2**). One can thus conclude that $[PtCl_4O]^{3-}$ is a good model for $[PtCl_4(OH)]^{2-}$ in terms of accounting for absorption in the 400–450-nm region.

However, a higher energy transition around 260 nm is also observed for the product of the reaction of OH and $[PtCl_4]^{2-}$. Here the $[PtCl_4O]^{3-}$ models proves to be inadequate in accounting for this band because it cannot provide another O p_σ level of greater stability (Figure 2). This can be achieved with the hydroxide system, as there is another O p_σ level (5a′), but owing to its bonding character, this level is very stable and the net difference between the two O p_σ levels (5a′ and 11a′ of Figure 2) is very substantial (32 500 cm^{-1}), so much so that if the lower energy transition is equated to the observed 455-nm band, then the intense higher energy transition will occur below 200 nm: this is not in agreement with experiment, which indicates a band in the region of 260 nm. The situation changes dramatically, however, if a water molecule

(37) In this analysis, the O 2s and Cl 3s orbitals have not been retained because they do not contribute significantly to the ligand MOs involved in the energy range of the observed CT bands.

(38) Day, P.; Sanders, N. J. *J. Chem. Soc. A* **1967**, 1536–1541.

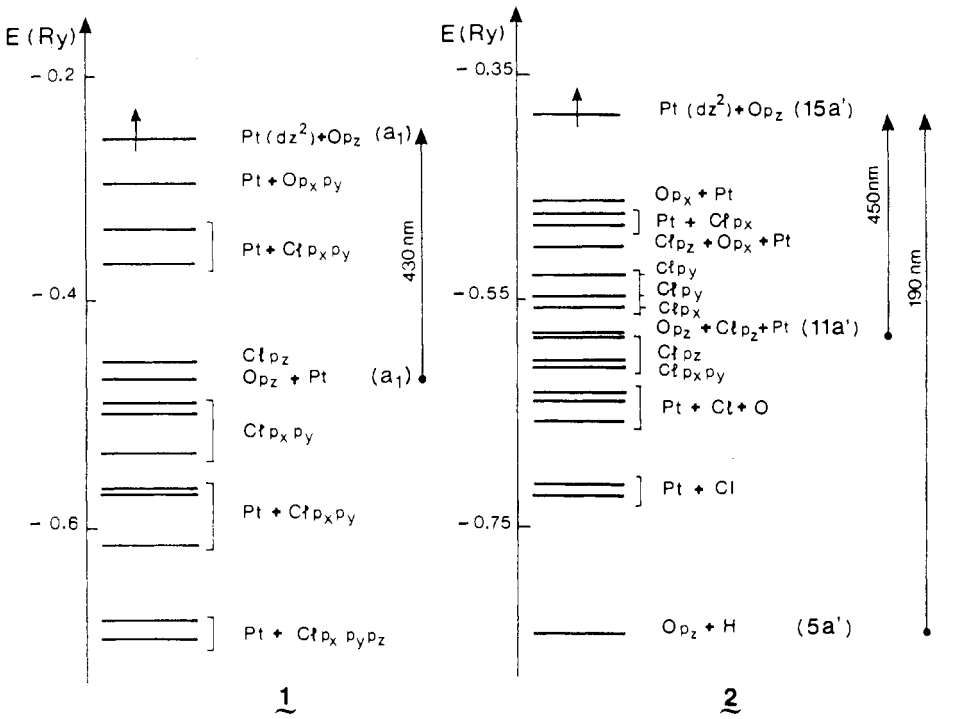

Figure 2. Energy level diagrams (upper valence part) for $[PtCl_4O]^{3-}$ and $[PtCl_4(OH)]^{2-}$ models. Pt–Cl = 2.48 Å; Pt–O = 2.30 Å.

Table I. Calculated CT Transitions for the $[PtCl_4O]^{3-}$ (**1**), $[PtCl_4(OH)]^{2-}$ (**2**), $[PtCl_4(OH)(H_2O)]^{2-}$ (**3**), and $[PtCl_4(OH)]^{2-}$ (**4**) Models

compd	sym-metry	CT type	CT value, nm
1	C_{4v}	O $p_z \rightarrow$ Pt d_{z^2}	430
		O p_z, H $\rightarrow$ Pt d_{z^2}	...
2	C_s	O $p_z \rightarrow$ Pt d_{z^2}	450
		O p_z, H $\rightarrow$ Pt d_{z^2}	190
3	C_s	O $p_z \rightarrow$ Pt d_{z^2}	450
			250 (Ow)[a]
		O p_z, H $\rightarrow$ Pt d_{z^2}	200
			150 (Ow)
4a	C_s	O p_z, Cl_3 $p_z \rightarrow$ Pt d_{z^2}, $d_{x^2-y^2}$	420
		Cl_4 p_y, Cl_5 $p_z \rightarrow$ Pt d_{z^2}, $d_{x^2-y^2}$	300
		Cl_3 p_z, $p_x \rightarrow$ Pt d_{z^2}, $d_{x^2-y^2}$	280
		Cl_3 p_z, $p_x \rightarrow$ Pt d_{z^2}, $d_{x^2-y^2}$	190
		O $p_z \rightarrow$ Pt d_{z^2}, $d_{x^2-y^2}$	180
4b	C_s	O $p_x \rightarrow$ Pt d_{xz}	540
		Cl_3 $p_z \rightarrow$ Pt d_{xz}	330
		Cl_3 $p_z \rightarrow$ Pt d_{xz}	290

[a] Ow means that the originating ligand level is localized on the oxygen of the water molecule.

is added to the sixth position of $[PtCl_4(OH)]^{2-}$ because now there are additional O $2p_\sigma$ levels. For $[PtCl_4(OH)(H_2O)]^{2-}$ (**3**), the calculations have been carried out for the C_s case with Pt–Cl = 2.48 Å and Pt–O = Pt–O(water) = 2.35 Å, and the energy level diagram is presented in Figure 3. As expected, two O p_σ levels are available (10a′ and 16a′), from which an electron can be transferred to the partially filled HOMO (18a′), and these two levels are separated by about 19 000 cm^{-1} in reasonable accord with the experimental findings. At greater energy stability, two bonding OH levels are encountered (6a′ and 8a′): for both sets of O p_σ levels, those related to OH are at higher energies than those pertaining to H_2O, and these features are retained for reasonable values of elongation for Pt–OH and Pt–OH_2 bond lengths. If the water molecule is replaced by a hydroxo ligand to give a *trans*-dihydroxo compound, the energy difference between the two available O p_σ levels of a′ symmetry is reduced to about 12 000 cm^{-1} from 19 000 cm^{-1} for the monoaquo system as the nature of the MOs is now changed. The calculated CT transitions for $[PtCl_4(OH)(H_2O)]^{2-}$ (**3**) are given in Table I.

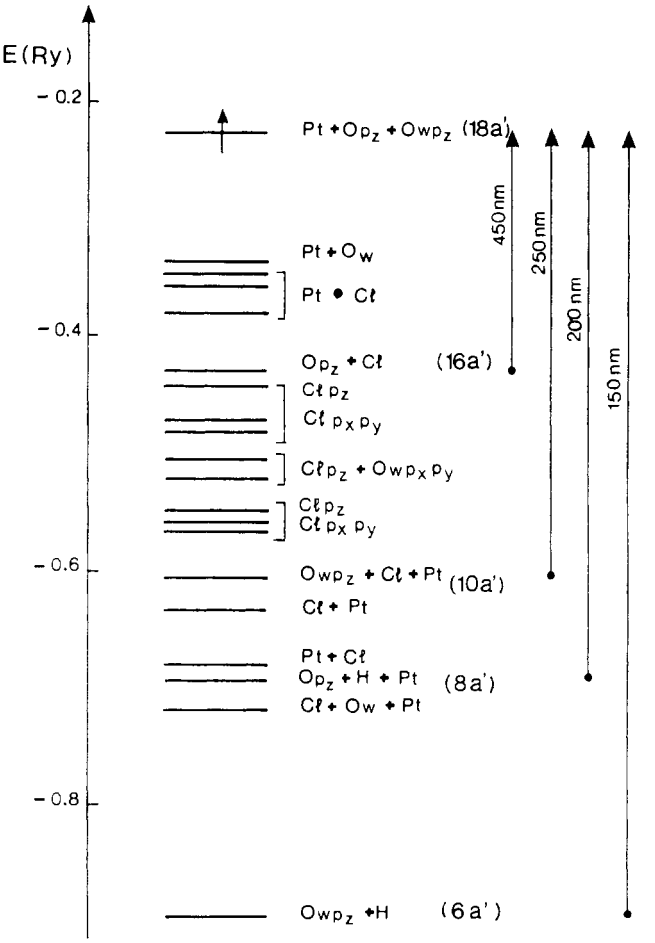

Figure 3. Energy level diagram (upper valence part) for the $[PtCl_4(OH)(H_2O)]^{2-}$ model. Pt–Cl = 2.48 Å; Pt–OH = Pt–OH_2 = 2.35 Å.

To complete this part, the $[PtCl_4(OH)]^{2-}$ model has also been studied in a pyramidal form with increased values of the Cl–Pt–OH bond angles. The results remain essentially unchanged for bond angles kept lower than 98°. A form of Berry rotation has been considered so as to allow the transformation of the

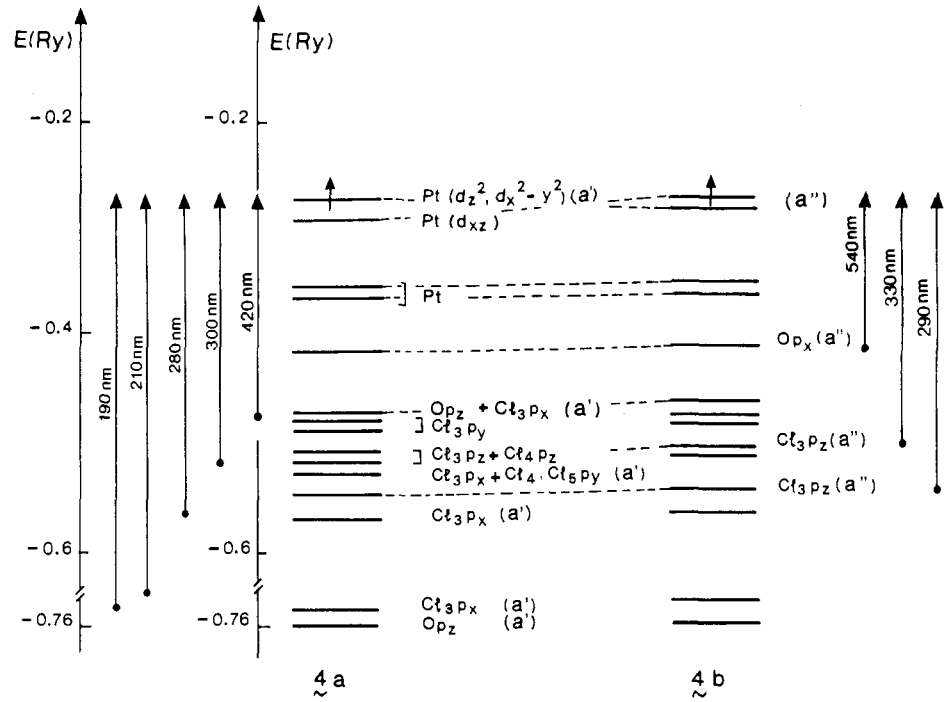

Figure 4. Energy level diagram (upper valence part) for the trigonal-bipyramidal form of the $[PtCl_4(OH)]^{2-}$ model: (a) Pt–O = 2.20 Å; (b) Pt–O = 2.25 Å, Pt–Cl = 2.32 Å.

square-pyramidal structure into a trigonal-bipyramidal one with the OH group as one of the three equatorial ligands, and the nonlinear Pt–O–H unit has been rotated so as to retain C_s symmetry. The energy level diagram is presented in Figure 4, and the two cases **4a** and **4b** are considered because the ground-state electronic structure is strongly dependent upon the Pt–OH bond length and the Cl–Pt–OH bond angles. Structure **4a** with a ground state of $^2A''$ occurs when the Pt–OH bond is kept shorter than 2.25 Å or the bond angle is smaller than 120°. Case **4b** arises if the bond is greater or equal to 2.25 Å or the Cl–Pt–OH angle is greater than or equal to 120°: the ground state is now $^2A'$.

The calculated positions of the CT transitions are given in Table I: case **4a** corresponds to the Pt–OH bond length of 2.20 Å, and for case **4b**, the Pt–OH and Pt–Cl bond lengths are 2.25 and 2.32 Å, respectively, with the Cl–Pt–OH angle being 120°. The change in the nature of the HOMO directly reflects the variation of the ligand field strength with geometry; such an effect is also apparent in the results of the EH calculations. Indeed, the HOMO of **4a** has mixed Pt d_{z^2} and $d_{x^2-y^2}$ character, while that of **4b** is Pt d_{xz}. For structure **4a**, the intense CT transitions will occur along the x, y, and z axes ($a' \rightarrow a'$), but for **4b**, they take place in the $x0z$ plane ($a'' \rightarrow a''$). Three CT transitions of $p_\sigma \rightarrow d_\sigma$ type (420, 300, and 190 nm) and two of mixed $p_\sigma + p_\pi \rightarrow d_\sigma$ type (280 and 210 nm) are expected for **4a**, whereas for structure **4b**, three CT transitions ($p_\pi \rightarrow d_\pi$) are anticipated (Table I). While bands are predicted in the 400–500-nm region, those around 300 nm are not found experimentally and thus these structures seem very improbable. These trigonal-bipyramidal structures and the aforementioned square-pyramidal one correspond to the types of structures proposed by Adams and co-workers to account for the longer lived transient with a peak near 410 nm and for the shorter lived one having a maximum near 450 nm that occur in the reaction of OH with $[PtCl_4]^{2-}$.[12] In view of our findings given above, these structures appear inadequate to explain the observed spectral features for the short-lived species. As proposed previously by us,[25] the hexacoordinated $[PtCl_4(OH)(H_2O)]^{2-}$ thus remains the only really viable candidate to account for the shorter lived transient having two intense absorption bands at 450 nm and near 260 nm.[18] In the next section, we consider candidates for the longer lived transient with a prominent peak at ca. 410 nm.

III. Models for the Longer Lived Transients. In mildly acidic solutions, the decay of the short-lived intermediate, proposed as $[PtCl_4(OH)(H_2O)]^{2-}$, is concomitant with the formation of a longer lived transient having a peak near 410 nm.[18] The accompanying conductivity increase (amounting to release of 1 equiv of proton) and the determination of the overall charge of the 410-nm transient as −1 point to the species being $[PtCl_2(OH)_2]^-$; however, at higher acidities or in basic media, the findings also suggest the occurrence of different but related complexes. To aid in the identification of the longer lived transients, investigations have been undertaken on the series of penta- and tetracoordinated models $[PtCl_3(OH)_2]^{2-}$, $[PtCl_3(OH)]^-$, $[PtCl_2(OH)_2]^-$, $[PtCl_2(OH)(H_2O)]$, and $[Pt(OH)_4]^-$.

***cis*- and *trans*-$[PtCl_3(OH)_2]^{2-}$ (5, 6).** The trans structure has its HOMO localized in the $x0z$ plane regardless of possible geometric distortions, and thus the Pt–OH bond length is not a significant parameter, whereas that for Pt–Cl is important. According to its value (whether being the same for all three chlorines or chosen differently), the ground state may be $^2A_1$ or $^2B_1$ with the HOMO having preponderant Pt d_{z^2} or d_{xz} character, respectively. But in all cases, both orbitals of a_1 and b_1 symmetries remain nearly degenerate; this comes from the fact that this structure is a quasi-D_{3h} case, analogous to one with an a'_1 HOMO. For the ligand orbitals to attain good overlap with Pt $5d_{xz}$ or $5d_{z^2}$, their MOs must have major contributions from the $Cl_3(p_x, p_z)$ and $Cl_4(p_x, p_z)$ orbitals (Figure 1). The transitions to be considered then will be $a_1 \rightarrow a_1$ ($^2A_1$ GS) or $a_1 \rightarrow b_1$ ($^2B_1$ GS). The calculated CT positions for three different geometries are presented in Table II. All involve two relatively close bands that might be experimentally observed as a single broad band; however, when this is also viewed in conjunction with the experimentally determined overall electrostatic charge on the transient of −1 as mentioned above, the possibility of this structure accounting for the 410-nm species seems remote. For the analogous cis complex, a C_{2v} model has been investigated. The HOMO here is of a_1 symmetry, and it has mixed Pt $d_{x^2-y^2}$ and d_{z^2} character. According to Day and Sanders' intensity criteria,[37] the appropriate excited state can involve $^2A_1$, $^2B_1$, and $^2B_2$ states (CT along the x, y, and z axes). A number of transitions with close energies are thus to be taken into account, and these are collected in Table II. While the results pertain to one set of bond lengths (Pt–Cl = 2.32 Å; Pt–OH = 2.25 Å), further elongation of the bonds will only introduce a red shift to the energies but it will not alter their number, and this point suffices to eliminate the cis form from further consideration.

$[PtCl_3(OH)]^-$, *cis*- and *trans*-$[PtCl_2(OH)_2]^-$, $[PtCl_2(OH)(H_2O)]$, and $[Pt(OH)_4]^-$. To investigate tetracoordinated strucutres,

Table II. Calculated CT Transitions of *trans*- and *cis*-$[PtCl_3(OH)_2]^{2-}$ Models[a]

	calcd CT transition, nm	bond lengths used, Å		
		Pt–Cl_3[a]	Pt–Cl_4[a]	Pt–OH
trans (**5**)	290	2.32	2.32	2.25
	250			
	370	2.53	2.53	2.25
	425			
	420	2.62	2.53	2.25
	450			
cis (**6**)	290			
	280			
	270	2.32	2.32	2.25
	260			
	235			
	170			

[a] See Figure 1 for numbering.

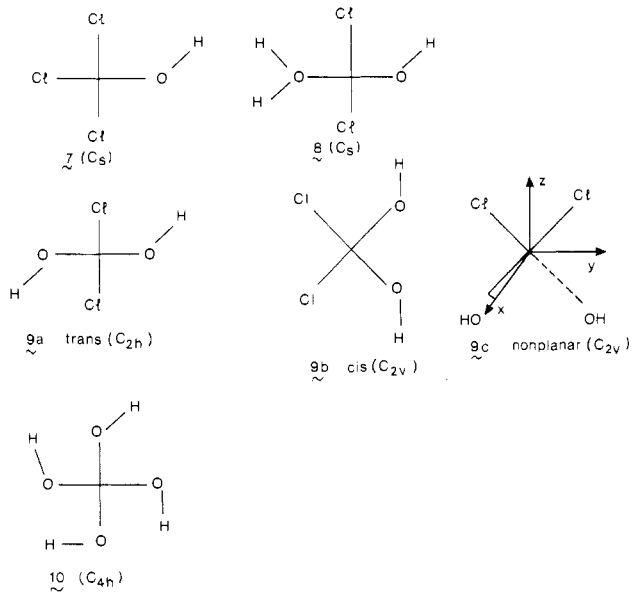

Figure 5. Tetracoordinated structures. Unless otherwise specified, the plane of the drawing is the $x0y$ plane.

standard and shortened Pt–OH and Pt–Cl distances have been adopted. For all of the species, square-planar forms have been considered, and a distorted-tetrahedral one has also been studied in the case of $[PtCl_2(OH)_2]^-$. Since variations of the in-plane bond angles for this latter complex have led to negligible shifts in the calculated CT transitions in a square-planar context, we have also used 90° for the other square-planar species. For all such species, the HOMO is a d_π orbital: the intense transitions will then be related to $p_\pi \rightarrow d_\pi$ changes. According to the particular symmetry adopted, there will be one or two transitions, and this supports the assumption that the long-lived transient with one intense band at 410 nm is likely to be of a square-planar variety.

For $[PtCl_3(OH)]^-$ (**7**) and $[PtCl_2(OH)(H_2O)]$ (**8**), the calculations have been carried out within C_s symmetry with the mirror plane ($x0y$) being the molecular plane (Figure 5). The HOMOs of both correspond to π antibonding interactions between the Pt $5d_{xy}$ and Cl $3p_{x,y}$ orbitals; thus, the energies are primarily dependent on the Pt–Cl bond lengths. For standard values of these bond lengths, the two intense a′ → a′ transitions (O p_π and Cl p_π to Pt $5d_{xy}$) are calculated to be at low energies: for $[PtCl_3(OH)]^-$, 660 and 610 nm. To shift the values of these transitions to the 410-nm region, shorter Pt–Cl distances must be used. With the Pt–Cl bonds at 2.11 Å, the two intense transitions for the trichloro comple are now predicted to be at 414 and 395 nm. Two similar transitions are obtained at 425 and 410 nm for $[PtCl_2(OH)(H_2O)]$ when the Pt–Cl bond lengths are taken as 2.20 Å. These values of Pt–Cl bond distances represent substantial contractions with respect to the standard lengths. For both **7** and **8**, the low symmetry allows the presence of two intense transitions. However, in each instance, they are sufficiently close in energy so as to occasion the possibility that the two transitions could appear as a single broad band: for the 410-nm band, the full width at half-maximum is 60 ± 5 nm.[18] While these models cannot be excluded, the experimental data generally point toward $[PtCl_2(OH)_2]^-$ as being a better candidate for the 410-nm band.

Table III. Calculated Intense CT Transitions of Planar Tetracoordinated Pt(III) Models (with Appropriate Pt–Cl and Pt–O Bond Lengths)

model	calcd CT transitions, nm	bond lengths used, Å	
		Pt–Cl	Pt–O
$[PtCl_4]^-$[a]	620	2.32	
	410		
$[PtCl_3OH]^-$ (**7**)	414	2.10	2.04
	395		
$[PtCl_2(OH)(H_2O)]$ (**8**)	425	2.20	2.04
	410		
trans-$[PtCl_2(OH)_2]^-$ (**9a**)	408	2.32	2.00
cis-$[PtCl_2(OH)_2]^-$ (**9b**)	415	2.32	1.96
$[Pt(OH)_4]^-$ (**10**)	415	2.32	2.04

[a] Reference 25.

With this system, nonplanar as well as planar forms have been considered. For the latter form, the potentiality for geometrical isomers occurs. The trans form (**9a**) has higher symmetry (C_{2h}) than that for the cis case (C_{2v}, **9b**), but associated with this in both models is a unique, intense CT transition, $6b_u \rightarrow 4b_g$ (trans) and $6b_2 \rightarrow 3a_2$ (cis). For the former, the calculated CT value is 408 nm when the Pt–OH bonds are contracted by 0.04 Å with respect to the standard value. A value of 415 nm is obtained for the cis structure with the Pt–OH bonds shortened by 0.08 Å. Clearly both cases are compatible with the experimental situation, and indeed it does not appear feasible on the basis of detection by visible absorption to distinguish between the presence of either one form alone or a mixture of the two.

The nonplanar structure (Figure 5, form **9c**) is found to exhibit three allowed transitions, two of the $b_2 \rightarrow b_2$ category and one of the $a_2 \rightarrow b_2$ type. On the basis of overlap considerations, the $4b_2 \rightarrow 5b_2$ and the $2a_2 \rightarrow 5b_2$ movements should be associated with the more intense bands and the $3b_2 \rightarrow 5b_2$ one would be less intense. The former are calculated to be at 420 and 418 nm, respectively, for standard bond lengths but with Cl–Pt–Cl and Cl–Pt–OH angles increased from 90 to 120°; that is, the two transitions are nearly degenerate for a tetrahedral-like structure, so they are expected to appear as one band with a maximum near the observed 410-nm peak. The less intense transition is predicted to occur at 340 nm; however, this is not discernible in the recorded spectra so that the nonplanar case seems considerably less favorable in accounting for the experimental observations than does the planar situation.

To complete the investigations of tetracoordinated square-planar species, the fully aquated form $[Pt(OH)_4]^-$ has been studied within the context of a rigid C_{4h} structure. According to the Jahn–Teller theorem, the ^2E_g ground state is unstable; however, one can imagine that OH rotations or small bond angle deformations can lower the symmetry to C_{2h} or C_{2v} without major changes occurring in the energy difference between the new HOMO (Pt $5d_{xz}$ or $5d_{yz}$) and the O p_π MOs related to the $3e_u$ orbital. For the C_{4h} condition (Figure 5, form **10**), the $3e_u \rightarrow 2e_g$ CT transition is calculated to be at 415 nm for standard Pt–OH bond lengths. Since we have found that OH rotations or bond angle changes up to 10° do not alter the locations of the CT transitions by more than 1000 cm^{-1}, $[Pt(OH)_4]^-$ is predicted to have a transition near 410 nm even after some Jahn–Teller distortion.

Table III collects the calculated CT transitions for the planar tetracoordinated structures investigated here and in the earlier study of $[PtCl_4]^-$.[24] Examination of these results indicates that

while the tetrachloro complex is no longer a probable candidate for the 410-nm transient, the aquated forms to varying degrees are realistic possibilities, including possibly cases such as $[PtCl(OH)_3]^-$ that have not been considered here. In general, then, the possibility exists, on the basis of these model studies, that the 410-nm band may not always be indicative of a single species or even the same one under different conditions, and in the following paper, we present the experimental results and compare them to those obtained here by the use of the Xα method.

Acknowledgment. These calculations have been performed at the CNUSC (Montpellier, France) and the CC-IN2P3 (Lyon, France). The financial support provided by the Natural Sciences and Engineering Research Council of Canada to W.L.W. and by the North Atlantic Treaty Organization (Project No. 0680/85) is very much appreciated.

Contribution from the Department of Chemistry and the Saskatchewan Accelerator Laboratory, University of Saskatchewan, Saskatoon, Saskatchewan S7N 0W0, Canada, Bereich Strahlenchemie, Hahn-Meitner-Institut, Postfach 39 01 28, D-1000 Berlin 39, Ecole de Chimie, 34075 Montpellier Cedex, France, and Institut de Physique Nucléaire (et IN2P3), Université de Lyon I, 68622 Villeurbanne Cedex, France

Photolytic and Radiolytic Study of Platinum(III) Complex Ions Containing Aquo and Chloro Ligands

W. L. Waltz,*[1a] J. Lilie,[1b] A. Goursot,[1c] and H. Chermette[1d]

Received July 22, 1988

The formations and characterizations of short-lived, monomeric platinum(III) complex ions containing aquo and chloro ligands have been studied by using pulse radiolysis and laser photolysis techniques coupled with UV–visible absorption and conductivity detection methods. Five different chemical routes have been used to generate in aqueous media the same or similar platinum(III) species: reaction of tetrachloroplatinum(II), $[PtCl_4]^{2-}$, with the hydroxyl radical, interactions of hexachloroplatinum(IV), $[PtCl_6]^{2-}$, with the hydrated electron, hydrogen atom, and *tert*-butyl alcohol radical, and the 265-nm photolysis of $[PtCl_6]^{2-}$ with the latter giving rise to both oxidation–reduction and ligand-substitution processes. The platinum(III) intermediates can be classified into two categories. The nascent or shorter lived species exhibit intense charge-transfer bands with peak maxima near 450 nm or at wavelengths below 300 nm, and they are proposed to be of a distorted-octahedral type with compositions of the form $[Pt^{III}(Cl)_{6-m}(X)_m]$ (m = 0–2; X = OH, H_2O). The longer lived Pt(III) complexes are characterized by a single charge-transfer band having a peak between 410 and 420 nm and by compositions of the type $[Pt^{III}(Cl)_{4-n}(X)_n]$ (n = 1–3; X = OH, H_2O) having limiting square-planar structures. The mechanisms for the formations of the platinum(III) complex ions and for their interrelationships are discussed, and evidence is presented to indicate that these species act as catalytic agents in the thermal aquation of $[PtCl_6]^{2-}$.

Introduction

A number of experimental investigations using fast reaction techniques coupled with UV–visible absorption detection have established that the radiolytic and photolytic reactions in aqueous media of octahedral hexachloroplatinum(IV) ion, $[PtCl_6]^{2-}$, and of the square-planar tetrachloroplatinum(II) complex, $[PtCl_4]^{2-}$, can give rise to transitory species characterized as monomeric platinum entities in which the metal center is in the unusual formal oxidation state of +3.[2-8] The reaction of the hydroxyl radical and $[PtCl_4]^{2-}$ yields as the nascently observed product a species with an absorption maximum near 450 nm that subsequently decays via a first-order rate law to generate a longer lived transient having a peak near 410 nm.[2,3] While earlier workers recognized the possibility that the initial process could involve an electron-transfer mechanism, they proposed that the process is one incorporating OH addition to the metal center to give the five-coordinate, square-pyramidal product $[PtCl_4(OH)]^{2-}$. Its subsequent intramolecular rearrangement to a trigonal-bipyramidal form is then associated with the absorption peak at 410 nm. The nascent absorption at 450 nm was, however, not observed at low or high pHs: in alkaline media, the indications were that both the initial and longer lived intermediates now exhibited peaks near 390 nm. No detailed explanations were offered to account for these acid–base effects even though they appear to be at variance with the proposed intramolecular mechanism.

The same or similar species absorbing at 410 nm (but none exhibiting a peak at 450 nm) have been observed in the reaction of the hydrated electron, e_{aq}^-, and $[PtCl_6]^{2-}$ and in the conventional flash photolysis of $[PtCl_6]^{2-}$.[2,4] More recent results, obtained by picosecond laser photolysis and interpreted with aid of theoretical calculations performed by using multiple-scattering MO Xα theory, clearly point to the initial photoredox product as being the short-lived, square-pyramidal $[PtCl_5]^{2-}$.[7] While here it was not feasible experimentally to determine the nature of the subsequent product(s) arising from the rapid decay of $[PtCl_5]^{2-}$ (τ = 210 ps), the probable implication would be that such could be the longer lived species (micro- to millisecond scales) absorbing at 450 and 410 nm.

A key observation in regard to the 410-nm transient and one that is consistent with its designation as a platinum(III) complex ion is its reaction with $Fe^{2+}(aq)$.[4] From the influence of ionic strength on this process, Wright and Laurence concluded that its overall electrostatic charge was −1. As this feature is not consistent with the charge of −2 for the species proposed by Adams and co-workers,[2] the former authors suggested that the 410-nm intermediate was $[PtCl_4]^-$, having a square-planar form with possibly two labile apical positions.[4] However, the validity of the overall charge measurement has been questioned.[6]

While these earlier studies have brought to light a number of intriguing features about platinum(III) chloro complexes, no consistent picture has yet emerged as to their compositions/structures or to their mechanistic interrelationships. Furthermore, the results of theoretical calculations do not in general support the 410- and 450-nm transients as being five-coordinate.[9-11] In

* To whom correspondence should be addressed.

(1) (a) University of Saskatchewan. (b) Hahn-Meitner-Institut. (c) Ecole de Chimie. (d) Université de Lyon I.
(2) Adams, G. B.; Broskiewicz, R. B.; Michael, B. D. *J. Chem. Soc., Faraday Trans. 1* **1968**, *64*, 1256–1264.
(3) Ghosh-Mazumdar, A. S.; Hart, E. J. *Int. J. Radiat. Phys. Chem.* **1969**, *1*, 165–176.
(4) Wright, R.; Laurence, G. S. *J. Chem. Soc., Chem. Commun.* **1972**, 132–133.
(5) Storer, D. K.; Waltz, W. L.; Brodovitch, J. C.; Eager, R. L. *Int. J. Radiat. Phys. Chem.* **1975**, *7*, 693–704.
(6) Broszkeiwicz, R. K.; Grodkowski, J. *Int. J. Radiat. Phys. Chem.* **1976**, *8*, 359–365.
(7) Goursot, A.; Kirk, A. D.; Waltz, W. L.; Porter, G. B.; Sharma, D. K. *Inorg. Chem.* **1987**, *26*, 14–18.
(8) Anbar, M.; Bamenek, M.; Ross, A. B. *Natl. Stand. Ref. Data Ser. (U.S., Natl. Bur. Stand.)* **1973**, *NSRDS-NBS43*.

0020-1669/89/1328-2247$01.50/0